Al-MCM-41 supported magnesium oxide as catalyst for synthesis of α-pentylcinnamaldehyde

Jui-I Yu, Shin Yi Shiau and An-Nan Ko *

Department of Chemistry, Tunghai Universty, Taichung, Taiwan, ROC

Received 5 March 2001; accepted 8 August 2001

The catalytic reaction of benzaldehyde with n-heptaldehyde was studied at 100–175 °C in a stirred batch autoclave reactor using mesoporous molecular sieve Al-MCM-41 supported MgO. Competitive reactions of cross- *versus* self-aldolization produce α-pentylcinnamaldehyde (α-P_C) and 2-pentyl-2-nonenal, respectively. Both reactions exhibit similar activation energies. Increasing the deposited amount of MgO on Al-MCM-41 enhances the catalyst base amount but diminishes the surface area. The conversion of n-heptaldehyde increases with catalyst base amount, reaction temperature and reaction time, whereas the α-P_C selectivity exhibits only small variation with reaction conditions. The catalytic activity of Al-MCM-41 is significantly enhanced by the deposition of MgO.

KEY WORDS: aldol condensation; Al-MCM-41 supported MgO; benzaldehyde; n-heptaldehyde; α-pentylcinnamaldehyde

1. Introduction

Despite extensive studies on heterogeneous acid catalysts, the application of base catalysts receives much less attention. However, interest has increased during the past two decades. A wide variety of reactions is base-catalyzed such as isomerization, dehydrogenation, alkylation, hydrogenation, amination, and aldol condensation [1]. Aldol condensation may occur *via* self-condensation between two of the same aldehyde or ketone molecules or *via* cross-condensation between two molecules of different aldehydes or ketones [2–10]. Acrylaldehyde was synthesized from vapor-phase aldolization of formaldehyde with acetaldehyde using various oxides supported on silica gel. The catalytic activity was enhanced by the incorporation of a basic or amphoteric oxide into the silica gel, whereas the reverse result was obtained when acidic oxides were deposited [8]. With oxides such as ZnO, MgO, MoO_3, B_2O_3, and P_2O_5 deposited on ZSM-5, Y-faujasite, Al_2O_3, and SiO_2, the best performance in the synthesis of acrylaldehyde from formaldehyde and acetaldehyde was attained using a 4 wt% MgO/ZSM-5 catalyst [9]. In the reaction between acetaldehyde and benzaldehyde to form 1-phenylpropene, reduced CeO_2 was observed to be active [10].

α-pentylcinnamaldehyde (α-P_c) has been used in perfumery and flavoring; it is traditionally manufactured from benzaldehyde and n-heptaldehyde in presence of sodium or potassium hydroxide [11]. However, the drawback of such a process includes corrosion, separation procedures and environmental problems due to the use of alkali metal hydroxides. Accordingly, this synthetic reaction has been carried out using solid base catalysts such as anionic exchange resins [12], solid–liquid phase transfer catalysts [13,14], organic–inorganic hybride catalysts and MCM-41 supported metal oxides [15]. For this reaction over the MCM-41 material containing the strong hindered amine base, the catalyst deactivated due to loss of the base at the higher reaction temperature and by poisoning of the strong basic sites with benzoic acid which was produced from the disproportionation of benzaldehyde. Instead, the K_2O/La_2O_3 incorporated MCM-41 can be used at a higher reaction temperature to attain greater intrinsic activity [15].

Recently, the mesoporous molecular sieve MCM-41 was developed and applied in many acid-catalyzed reactions [16, 17]. However, up to now much fewer works on its role as a base catalyst have been reported [15,18]. In this study, MgO was deposited on Al-MCM-41 in order to prepare catalysts with enhanced basicity. Liquid phase aldolization between benzaldehyde and n-heptaldehyde to form α-pentylcinnamaldehyde was investigated using MgO and Al-MCM-41 supported MgO. The effects of reaction temperature, pressure, and benzaldehyde/n-heptaldehyde molar ratio (B/H) were studied. The catalytic results were correlated to catalyst properties. In addition, other aliphatic aldehydes were utilized to compare their catalytic activities and product selectivities over the MgO catalyst. The reaction mechanism for the formation of α-alkylcinnamaldehyde was proposed.

2. Experimental

Magnesium oxide (Strem) was calcined at 600 °C for 6 h before use. Al-MCM-41 was prepared from sodium aluminate (RDH), sodium silicate (Aldrich), sulfuric acid (RDH) and cetyltrimethylammonium bromide (RDH), following the procedures given in [19]. To prepare MgO/Al-MCM-41, appropriate amount of magnesium acetate (RDH) was dissolved in 30 ml deionized water. Then 5 g of Al-MCM-41 was added with stirring into the above solution.

---

* To whom correspondence should be addressed.

After drying in a desiccator, the catalyst was heated at 110 °C for 12 h and finally calcined at 500 °C for 4 h.

The X-ray diffraction patterns of various powder samples were measured with a diffractometer (Shimadzu XD-5). The Si/Al mol ratio in the bulk sample of Al-MCM-41 was determined with an ICP-AES (Allied Analytical ICAP 9000). The BET surface area and the adsorption–desorption isotherm were obtained with a gas sorption analyzer (Micromeritics ASAP 2000). The ^{27}Al and ^{29}Si MAS-NMR spectra of Al-MCM-41 samples were recorded (Bruker DSX 400 WB). The temperature-programmed desorption of carbon dioxide from various catalysts was performed in the range of 100–600 °C, following the procedures described in [20].

The catalyst (0.2 g) was added into a solution mixture (35 ml) of benzaldehyde (RDH) and n-heptaldehyde (RDH) with different B/H molar ratios. The reaction was carried out in a stirred batch autoclave reactor (100 ml, Autoclave Engineering, Inc.) at 100–175 °C for 2 h. The reaction products were identified with a GC-MS (Hitachi M-52) and analyzed by a gas chromatograph (HP 5890 series II) using a flame-ionization detector and a PONA capillary column (50 m × 0.2 mm).

3. Results and discussion

The Si/Al mol ratio in the Al-MCM-41 sample is 25.0 according to ICP-AES analysis. Figure 1 shows a typical example of the powder X-ray diffraction patterns of Al-MCM-41 and 20 wt% MgO/Al-MCM-41. The as-synthesized Al-MCM-41 sample (figure 1, curve (a)) exhibits a strong peak at a d-spacing of 37.2 Å and two weak peaks at those of 22.6 and 19.8 Å. After calcination, the d-spacing of these three peaks decreases with concomitant increase in their peak intensities (figure 1, curve (b)). Such well-defined pattern is typical of Al-MCM-41 [21,22]. The deposition of 20% MgO on Al-MCM-41 causes apparent decrease of the peak intensities. However, the sample still exhibits characteristic hexagonal structure (figure 1, curve (c)).

Figure 2 compares N_2 adsorption–desorption isotherms between Al-MCM-41 and 20% MgO/Al-MCM-41. Both samples exhibit type IV adsorption curves, which are characteristic of mesoporous solids [21]. In addition, the samples display a hysteresis loop in the region of P/P_0 above 0.4; such a hysteresis is assigned to the capillary condensation in the mesopores [23]. Although the pore sizes are similar, both the BET surface area and the pore volume diminish significantly upon deposition of MgO, that is attributed to the blockage of pores. Such a result also leads to the decrease of XRD peak intensity. Figure 3 shows the ^{27}Al and ^{29}Si MAS-NMR spectra of various samples of Al-MCM-41 and MgO/Al-MCM-41. For the spectrum of as-synthesized Al-MCM-41, the peak at 53 ppm corresponds to tetrahedral coordinated structural aluminum (figure 3(A), curve (a)). A new peak at 0.7 ppm appears after

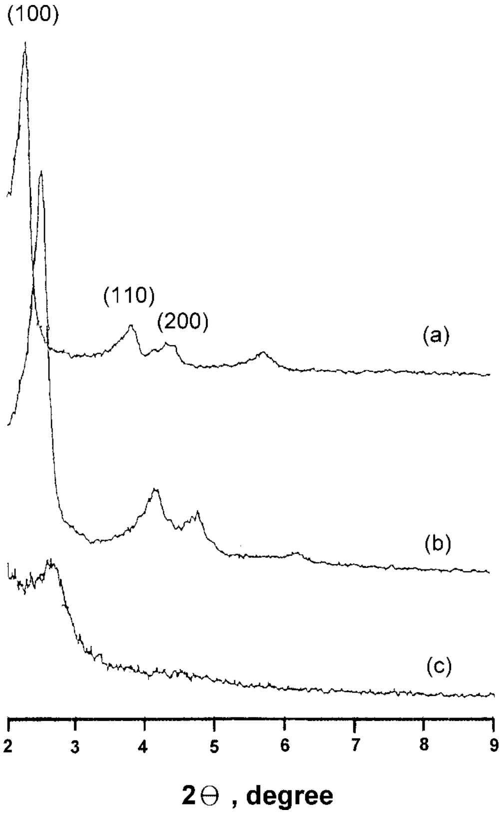

Figure 1. XRD powder patterns of Al-MCM-41: (a) as-synthesized, (b) calcined and (c) 20% MgO deposited.

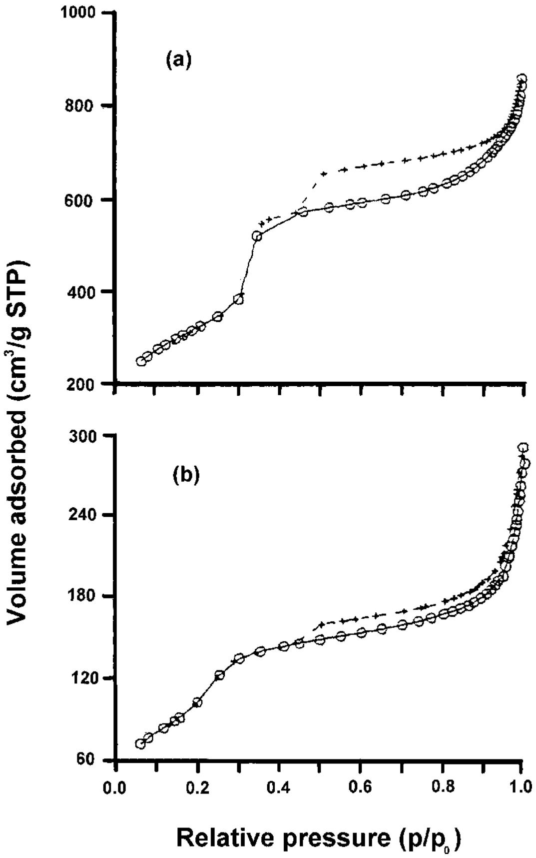

Figure 2. N_2 adsorption–desorption isotherms of calcined (a) Al-MCM-41 and (b) 20% MgO/Al-MCM-41.

calcination (figure 3(A), curve (b)) that is ascribed to the aluminum expelled from the Al-MCM-41 framework [24]. After deposition with different amounts of MgO, the spectra display only minor differences of both signal position and intensity (figure 3(A), curves (c)–(e)). With the ^{29}Si MAS-NMR spectra, all samples exhibit broad peaks which resemble that of amorphous silica (figure 3(B)). Q^n is usually used to represent $Si(OSi)_n(OH)_{4-n}$ in the environment of silicon in the skeletal structure of molecular sieves. For the as-synthesized Al-MCM-41, three resonances (Q^2–Q^4) are observed at −92, −101 and −110 ppm, respectively (figure 3(B), curve (a)) [25]. Calcination causes the apparent decrease of Q^3 peak intensity due to dehydration occurring on the surface of Si–OH (figure 3(B), curves (b)). Increasing the amount of MgO deposited on Al-MCM-41 results in the relative increase of Q^2 and Q^3 peak intensities (figure 3(B), curves (c)–(e)). Figure 4 shows the temperature-programmed desorption of CO_2 profiles from MgO and MgO/Al-MCM-41 samples. The catalyst base amount of Al-MCM-41 enhances apparently with the deposited amount of MgO.

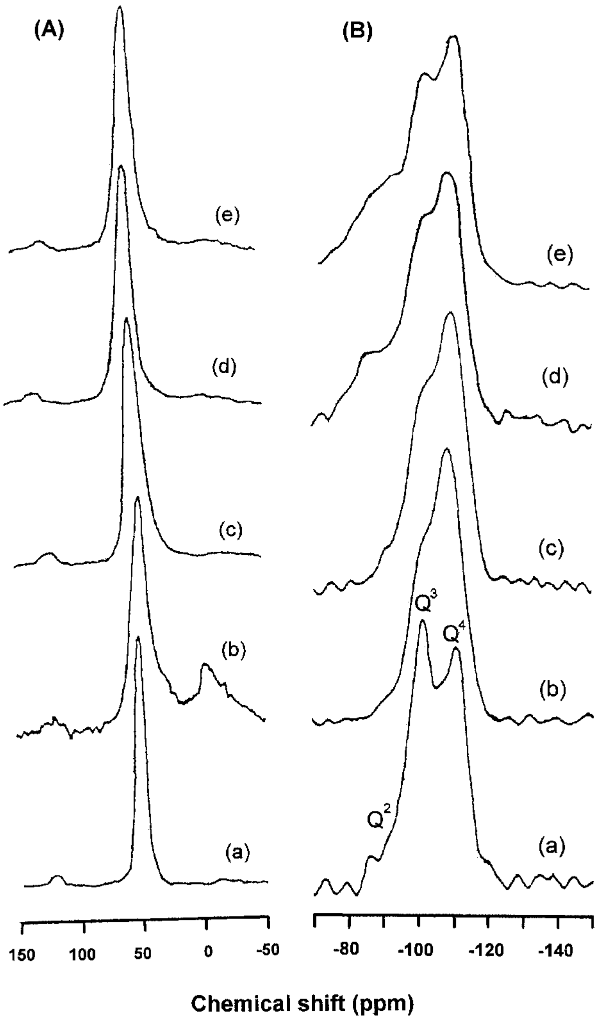

Figure 3. ^{27}Al (A) and ^{29}Si (B) MAS-NMR spectra of Al-MCM-41: (a) as-synthesized, (b) calcined, (c) 5% MgO, (d) 15% MgO and (e) 20% MgO.

In the reaction of benzaldehyde (B) with n-heptaldehyde (H), the products include α-pentylcinnamaldehyde (α-P_c) and 2-pentyl-2-nonenal (2P2N). Both the conversion (X) and the product selectivity (S) are calculated according to the mol of n-heptaldehyde converted,

$$X\ (\text{mol\%}) = \frac{\text{mol of } n\text{-heptaldehyde converted}}{\text{mol of } n\text{-heptaldehyde in the feed}} \times 100\%,$$

$$S_{\alpha\text{-Pc}}(\text{mol\%}) = \frac{\text{mol of } \alpha\text{-P}_\text{c}}{\text{mol of } n\text{-heptaldehyde converted}} \times 100\%,$$

$$S_{\text{2P2N}}\ (\text{mol\%}) = \frac{2(\text{mol of 2P2N})}{\text{mol of } n\text{-heptaldehyde converted}} \times 100\%.$$

To ensure the reaction to be free of diffusional limitation, the effect of stirring speed was investigated. It was found that the n-heptaldehyde conversion remained nearly the same at 700 and 900 rpm. Consequently, all experiments were performed at a speed of 900 rpm that caused no diffusion limitation. Figure 5 shows the influence of B/H mol ratio on the catalytic results over MgO catalyst at 150 °C. Increasing the B/H values results in an apparent increase of α-P_c selectivity, whereas only small change occurs in the conversion of n-heptaldehyde. As this is a competitive reaction system, *viz.* cross-aldolization between benzaldehyde and n-heptaldehyde *versus* self-aldolization of n-heptaldehyde, the low α-P_c selectivity of 13.3% at a B/H value of 1 implies the relatively faster reaction rate of self-aldolization of n-heptaldehyde. Accordingly, excess amount of benzaldehyde favors the formation of α-P_c. In the following experiments, the B/H mol ratio of 10 was chosen so as to obtain the higher α-P_c selectivity.

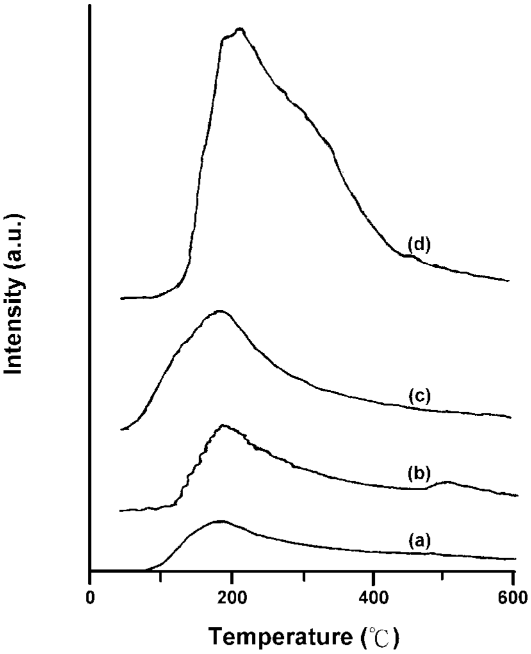

Figure 4. TPD of carbon dioxide profile from various catalysts: (a) 5% MgO/Al-MCM-41, (b) 15% MgO/Al-MCM-41, (c) 20% MgO/Al-MCM-41 and (d) MgO.

Table 1
Catalytic properties and catalytic results.[a]

Catalyst	Weight of MgO (g)	BET area (m^2/g)	Base amount mmol CO_2/g	Conversion (mol%) 1 h	Conversion (mol%) 2 h	α-P_C selectivity (mol%) 1 h	α-P_C selectivity (mol%) 2 h
Al-MCM-41	0	1032	–	7.2	9.4	40.7	41.6
5% MgO/Al-MCM-41	0.01	739	0.09	8.7	10.5	39.8	40.8
15% MgO/Al-MCM-41	0.026	726	0.11	14.2	20.5	38.8	39.5
20% MgO/Al-MCM-41	0.033	634	0.18	21.9	30.7	38.6	40.2
MgO	0.2	56	0.40	68.9	96.7	50.9	56.2

[a] Reaction conditions: B 336 mmol, H 33.6 mmol, catalyst 0.2 g, 150 °C, ambient pressure.

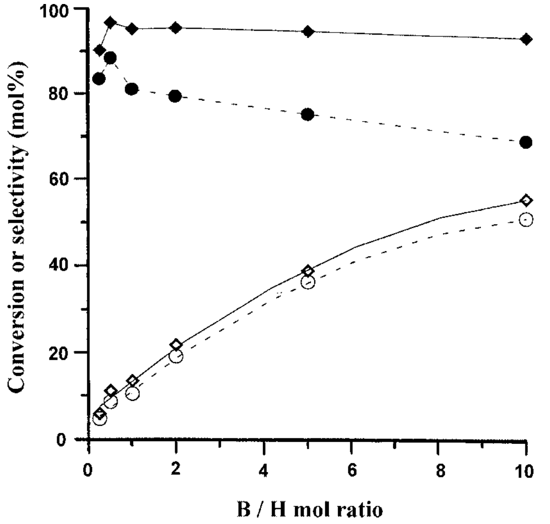

Figure 5. Effects of B/H mol ratio on the catalytic results over MgO catalyst at 150 °C. Conversion: (•) 1 and (♦) 2 h. α-P_c selectivity: (○) 1 and (◊) 2 h.

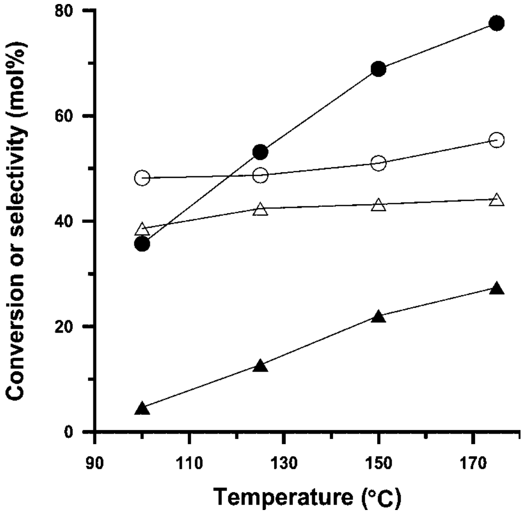

Figure 6. Effects of reaction temperature on the catalytic results after 2 h reaction. Conversion: (•) MgO and (▲) 20% MgO/Al-MCM-41. Selectivity: (○) MgO and (△) 20% MgO/Al-MCM-41.

Table 1 lists BET surface area, base amount, and catalytic results over various catalysts. As the amount of MgO deposited on Al-MCM-41 is increased, the catalyst base amount also increases markedly but with concomitant decrease in the surface area. Although Al-MCM-41 exhibits catalytic activity, its performance is significantly enhanced by the deposition of MgO. Furthermore, the catalytic activity correlates well with the catalyst base amount, whereas the α-P_c selectivity remains stable. The enhanced basic character of MgO on Al-MCM-41 is also evidenced by other base-catalyzed reactions such as the conversion of *n*-heptaldehyde or acetone.

Figure 6 shows the influence of reaction temperature on the catalytic results for reactions over 20% MgO/Al-MCM-41 and MgO. With an increase of temperature, the *n*-heptaldehyde conversion enhances apparently, whereas the α-P_c selectivity only increases slightly. This infers that the two competitive reactions, *viz.* self- and cross-aldolization, have similar activation energies. To investigate the effect of reaction pressures, the pressure in the reactor was adjusted by feeding the helium gas of 99.99% purity. Increasing the pressure causes a slight decrease of the *n*-heptaldehyde conversion but the α-P_c selectivity remains nearly unchanged. Aliphatic aldehydes, other than *n*-heptaldehyde, were also utilized to compare their catalytic results. Table 2 shows the catalytic activity and the product selectivity over the MgO catalyst. The conversion of aliphatic aldehydes increases with the carbon number of aliphatic aldehydes and the reaction temperature, whereas the selectivity of α-alkylcinnamaldehyde exhibits no clear trend. Scheme 1 illustrates the proposed reaction mechanism for the formation of α-alkylcinnamaldehyde. The catalyst basic sites abstract a proton from the α-carbon of aliphatic aldehyde to form carbanion I (step 1), which attacks the carbonyl carbon of benzaldehyde to form carbanion II (step 2). Carbanion II then abstracts a proton on the basic sites (step 3), followed by a proton transfer from catalyst acid sites and then dehydration to produce α-P_c (steps 4 and 5).

Table 2
Catalytic results in the reactions of benzaldehyde with different aliphatic aldehydes over MgO.[a]

Aliphatic aldehyde	Conversion (mol%) 125 °C	Conversion (mol%) 150 ° C	α-P_C selectivity (mol%) 125 °C	α-P_C selectivity (mol%) 150 °C
n-C_3H_7CHO	31.2	34.6	36.2	37.2
n-C_4H_9CHO	45.2	59.8	51.4	52.6
n-$C_5H_{11}CHO$	52.8	57.8	40.8	44.9
n-$C_6H_{13}CHO$	57.7	61.2	40.6	45.9
n-$C_7H_{15}CHO$	72.0	75.1	40.8	41.7

[a] Reaction conditions: benzaldehyde/aliphatic aldehyde = 10, 0.5 h, ambient pressure.

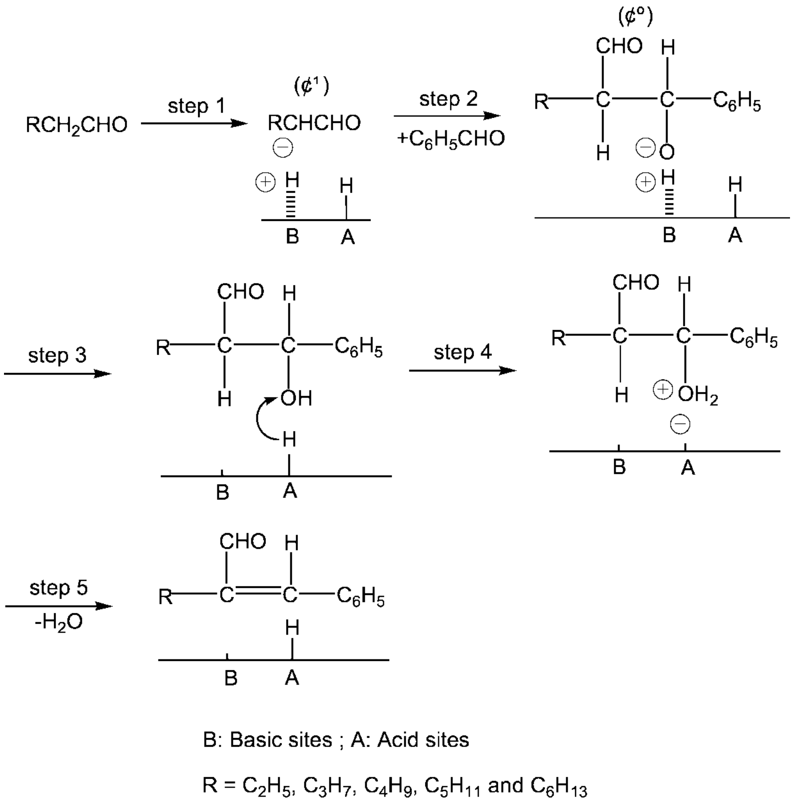

Scheme 1.

4. Conclusion

The molecular sieve Al-MCM-41 supported MgO exhibits characteristic mesoporous structures and acidic–basic properties. Increasing the deposited amount of MgO on Al-MCM-41 enhances the catalyst basicity but with a concomitant decrease of surface areas. In the reaction of benzaldehyde with aliphatic aldehydes, the aldehyde conversion increases remarkably with catalyst base amount, reaction temperature, reaction time and the chain length of aliphatic aldehydes, whereas the α-alkylcinnamaldehyde selectivity remains stable with temperature, time, and pressure of reactions. A promotive effect of catalytic activity occurs with the deposition of MgO on the mesoporous molecular sieve Al-MCM-41.

Acknowledgement

This work was supported by the National Science Council of the Republic of China (NSC 87-2113-M-029-005). We are grateful to Professor K.J. Chao of National Tsing Hua University for her comments and discussion.

References

[1] H. Hattori, Chem. Rev. 95 (1995) 537.
[2] H. Idriss, C. Diagne, J.P. Hindermann, A. Kiennemann and M.A. Barteau, J. Catal. 155 (1995) 219.
[3] W. Ji, Y. Chen and H.H. Kung, Appl. Catal. A 161 (1997) 93.
[4] Y.-C. Chang and A.-N. Ko, Appl. Catal. A 190 (2000) 149.
[5] W.T. Reichle, J. Catal. 94 (1985) 547.
[6] S. Lippert, W. Baumann and K. Thomke, J. Mol. Catal. 69 (1991) 199.
[7] H. Tsuji, F. Yagi, H. Hattori and H. Kita, J. Catal. 148 (1994) 759.
[8] M. Ai, Bull. Chem. Soc. Jpn. 64 (1991) 1342.
[9] E. Dumitriu, V. Hulea, N. Bilba, G. Carja and A. Azzouz, J. Mol. Catal. 79 (1993) 175.
[10] H. Idriss, M. Libby and M.A. Barteau, Catal. Lett. 15 (1992) 13.
[11] L.S. Payne, EP 0 392 579 A2 (1990).
[12] P. Mastagli and G. Durr, Bull. Soc. Chim. France 268 (1955).
[13] A. Sarkar, P.K. Dey and K. Datta, Indian J. Chem. B 25 (1986) 656.
[14] D. Abenhaim, C.P. Ngoc Son, A. Loupy and N. Ba Hiep, Synth. Commun. 24 (1994) 1199.
[15] S. Jaenicke, G.K. Chuah, X.H. Lin and X.C. Hu, Micropor. Mesopor. Mater. 35–36 (2000) 143.
[16] C.T. Kresge, M.E. Leonowicz, W.J. Roth, J.C. Vartuli and J.S. Beck, Nature 359 (1992) 710.
[17] X.S. Zhao, G.Q. Lu and G.J. Millar, Ind. Eng. Chem. Res. 35 (1996) 2075.
[18] A. Corma, S. Iborra and S. Miquel, J. Catal. 173 (1998) 315.
[19] H.P. Lin, S. Cheng and C.-Y. Mou, J. Chin. Chem. Soc. 43 (1996) 375.
[20] A.-N. Ko, C.-L. Yang, W.-D. Zhu and H.-E. Lin, Appl. Catal. A 134 (1996) 53.
[21] C.-Y. Chen, H.-X. Li and M.E. Davis, Micropor. Mater. 2 (1993) 17.
[22] A. Corma, V. Fornes, M.T. Navarro and J. Perez-Pariente, J. Catal. 148 (1994) 569.
[23] S.J. Gregg and K.S.W. Sing, *Adsorption, Surface Area and Porosity* (Academic Press, London, 1982).
[24] C.-F. Cheng and J. Klinowski, J. Chem. Soc. Faraday Trans. 92 (1996) 289.
[25] A. Liepold, K. Roos, W. Reschetilowski, A.P. Esculcas, J. Rocha, A. Philippou and M.W. Anderson, J. Chem. Soc. Faraday Trans. 92 (1996) 4623.